

Kavli IPMU - RIKEN iTHES - Osaka TSRP Symposium

"Frontiers of Theoretical Science - MATTER, LIFE and COSMOS -"

Vortex loops in hexagonal rare-earth manganites (RMnO_3) and the Kibble-Zurek mechanism

(to appear in Nature Physics)

Yoshitomo Kamiya

iTHES / Furusaki CMT Lab., RIKEN



Collaborators :

Theory : Shi-Zeng Lin, Gia-Wei Chern,
Wojciech Zurek, and Cristian Batista

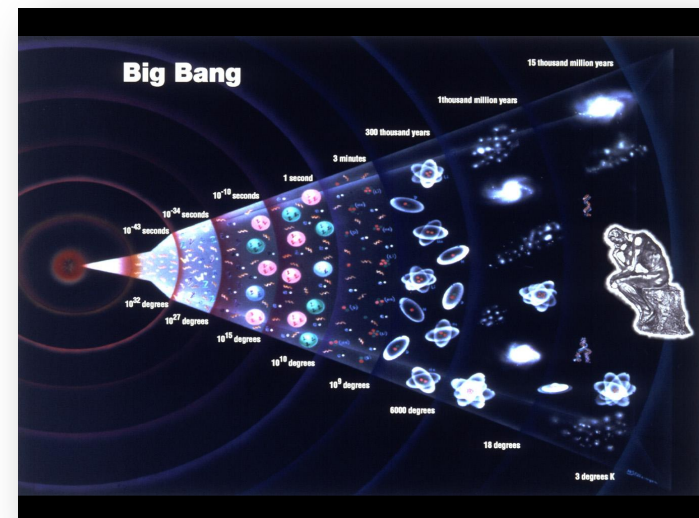
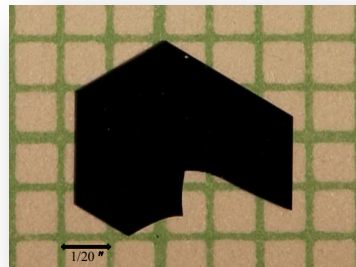


Experiments : S.-W. Cheong group & V. Kiryukhin group



Outline

- Hexagonal rare-earth manganites (RMnO_3) and the "trimerization" (structural transition) inducing ferroelectricity
- Visualization of frozen vortex loops
- Theoretical modeling with a 6-state "clock spin" (Z_6) model in 3D
 - Emergent symmetry at the critical point : $\text{Z}_6 \rightarrow \text{U}(1)$
 - Dual (vortex-loop) description of the phase transition
- Comparison with the Kibble-Zurek theory



As R (rare earth) of RMnO_3 , one may choose ...

5	37 Rb Rubidium 85.4678 [Xe]5s ¹	38 Sr Strontium 87.62 [Kr]5s ²	39 Y Yttrium 88.905 85 [Kr]4d ¹ 5s ²	40 Zr Zirconium 91.224 [Kr]4d ² 5s ²	41 Nb Niobium 92.906 38 [Kr]4d ⁴ 5s ¹	42 Mo Molybdenum 95.94 [Kr]4d ⁵ 5s ¹	43 Tc Technetium (98) [Kr]4d ⁵ 5s ¹	44 Ru Ruthenium 101.07 [Kr]4d ⁷ 5s ¹	45 Rh Rhodium 102.905 50 [Kr]4d ⁸ 5s ¹	46 Pd Palladium 106.42 [Kr]4d ¹⁰	47 Ag Silver 107.8682 [Kr]4d ¹⁰ 5s ¹	48 Cd Cadmium 112.411 [Kr]4d ¹⁰ 5s ²	49 In Indium 114.818 [Kr]4d ¹⁰ 5s ² 5p ¹	50 Sn Tin 118.710 [Kr]4d ¹⁰ 5s ² 5p ²	51 Sb Antimony 121.760 [Kr]4d ¹⁰ 5s ² 5p ³	52 Te Tellurium 127.60 [Kr]4d ¹⁰ 5s ² 5p ⁴	53 I Iodine 126.904 47 [Kr]4d ¹⁰ 5s ² 5p ⁵	54 Xe Xenon 131.293 [Kr]4d ¹⁰ 5s ² 5p ⁶
6	55 Cs Cesium 132.905 4519 [Xe]6s ¹	56 Ba Barium 137.327 [Xe]6s ²	57 La Lanthanum 138.905 47 [Xe]5d ¹ 6s ²	72 Hf Hafnium 178.49 [Xe]4f ¹⁴ 5d ² 6s ²	73 Ta Tantalum 180.947 88 [Xe]4f ¹⁴ 5d ³ 6s ²	74 W Tungsten 183.84 [Xe]4f ¹⁴ 5d ⁴ 6s ²	75 Re Rhenium 186.207 [Xe]4f ¹⁴ 5d ⁵ 6s ²	76 Os Osmium 190.23 [Xe]4f ¹⁴ 5d ⁶ 6s ²	77 Ir Iridium 192.217 [Xe]4f ¹⁴ 5d ⁷ 6s ²	78 Pt Platinum 195.084 [Xe]4f ¹⁴ 5d ⁹ 6s ¹	79 Au Gold 196.966 569 [Xe]4f ¹⁴ 5d ¹⁰ 6s ¹	80 Hg Mercury 200.59 [Xe]4f ¹⁴ 5d ¹⁰ 6s ²	81 Tl Thallium 204.38 [Xe]4f ¹⁴ 5d ¹⁰ 6s ² 6p ¹	82 Pb Lead 207.2 [Xe]4f ¹⁴ 5d ¹⁰ 6s ² 6p ²	83 Bi Bismuth 208.980 40 [Xe]4f ¹⁴ 5d ¹⁰ 6s ² 6p ³	84 Po Polonium (209) [Xe]4f ¹⁴ 5d ¹⁰ 6s ² 6p ⁴	85 At Astatine (210) [Xe]4f ¹⁴ 5d ¹⁰ 6s ² 6p ⁵	86 Rn Radon (222) [Xe]4f ¹⁴ 5d ¹⁰ 6s ² 6p ⁶
7	87 Fr Francium (223) [Rn]7s ¹	88 Ra Radium (226) [Rn]7s ²	89 Ac Actinium (227) [Rn]6d ¹ 7s ²	104 Rf Rutherfordium (261) [Rn]5f ¹⁴ 6d ² 7s ²	105 Db Dubnium (262) [Rn]5f ¹⁴ 6d ³ 7s ²	106 Sg Seaborgium (266) [Rn]5f ¹⁴ 6d ⁴ 7s ²	107 Bh Bohrium (264) [Rn]5f ¹⁴ 6d ⁵ 7s ²	108 Hs Hassium (277) [Rn]5f ¹⁴ 6d ⁶ 7s ²	109 Mt Meitnerium (268) [Rn]5f ¹⁴ 6d ⁷ 7s ²	110 Ds Darmstadtium (271) [Rn]5f ¹⁴ 6d ⁸ 7s ¹	111 Rg Roentgenium (272) [Rn]5f ¹⁴ 6d ⁹ 7s ¹	112 Cn Copernicium (285) [Rn]5f ¹⁴ 6d ¹⁰ 7s ²	113 Uut*	114 Uuq*	115 Uup*	116 Uuh*	117 Uus*	118 Uuo*

* The systematic names and symbols for elements greater than 112 will be used until the approval of trivial names by IUPAC.

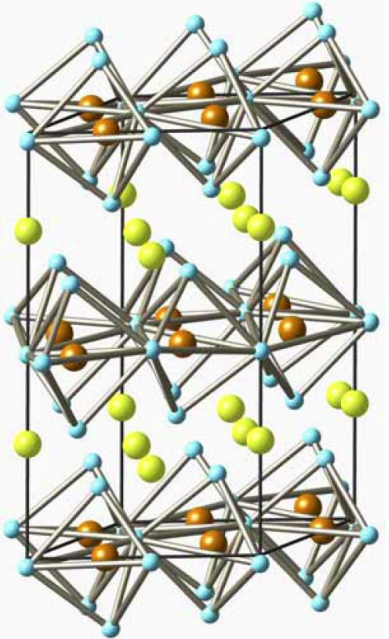
The discoveries of elements with atomic numbers 113–118 have been reported but not fully confirmed.

Elements whose average atomic masses appear bolded and italicized are recognized by the International Union of Pure and Applied Chemistry (IUPAC) to have several stable isotopes. Thus, the average atomic mass for each of these elements is officially expressed as a range of values. A range of values expresses that the average atomic mass of a sample of one of these elements is not depending on the history of the element. However, the

58 Ce Cerium 140.116 [Xe]4f ¹ 5d ¹ 6s ²	59 Pr Praseodymium 140.907 65 [Xe]4f ³ 6s ²	60 Nd Neodymium 144.242 [Xe]4f ⁴ 6s ²	61 Pm Promethium (145) [Xe]4f ⁵ 6s ²	62 Sm Samarium 150.36 [Xe]4f ⁶ 6s ²	63 Eu Europium 151.964 [Xe]4f ⁷ 6s ²	64 Gd Gadolinium 157.25 [Xe]4f ⁷ 5d ¹ 6s ²	65 Tb Terbium 158.925 35 [Xe]4f ⁹ 6s ²	66 Dy Dysprosium 162.500 [Xe]4f ¹⁰ 6s ²	67 Ho Holmium 164.930 32 [Xe]4f ¹¹ 6s ²	68 Er Erbium 167.259 [Xe]4f ¹² 6s ²	69 Tm Thulium 168.934 21 [Xe]4f ¹³ 6s ²	70 Yb Ytterbium 173.04 [Xe]4f ¹⁴ 6s ²	71 Lu Lutetium 174.967 [Xe]4f ¹⁴ 5d ¹ 6s ²
90 Th Thorium (232) [Rn]6d ² 7s ²	91 Pa Protactinium (231) [Rn]5f ² 6d ¹ 7s ²	92 U Uranium (238) [Rn]5f ³ 6d ¹ 7s ²	93 Np Neptunium (237) [Rn]5f ⁴ 6d ¹ 7s ²	94 Pu Plutonium (244) [Rn]5f ⁶ 6d ¹ 7s ²	95 Am Americium (243) [Rn]5f ⁷ 6d ¹ 7s ²	96 Cm Curium (247) [Rn]5f ⁷ 6d ¹ 7s ²	97 Bk Berkelium (247) [Rn]5f ⁹ 6d ¹ 7s ²	98 Cf Californium (251) [Rn]5f ¹⁰ 6d ¹ 7s ²	99 Es Einsteinium (252) [Rn]5f ¹¹ 6d ¹ 7s ²	100 Fm Fermium (257) [Rn]5f ¹² 6d ¹ 7s ²	101 Md Mendelevium (258) [Rn]5f ¹³ 6d ¹ 7s ²	102 No Nobelium (259) [Rn]5f ¹⁴ 6d ¹ 7s ²	103 Lr Lawrencium (262) [Rn]5f ¹⁴ 6d ¹ 7s ²

Perovskite RMnO_3

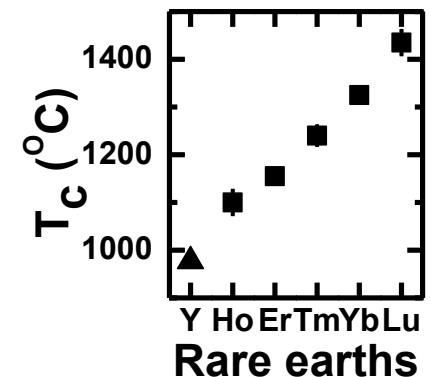
Hexagonal RMnO_3



Common properties

- Ferroelectric insulators
- $T_c > \sim 1300$ K
- $T_N \sim 100$ K (*)

FE transition T



(* We are not concerned about magnetism in this talk)

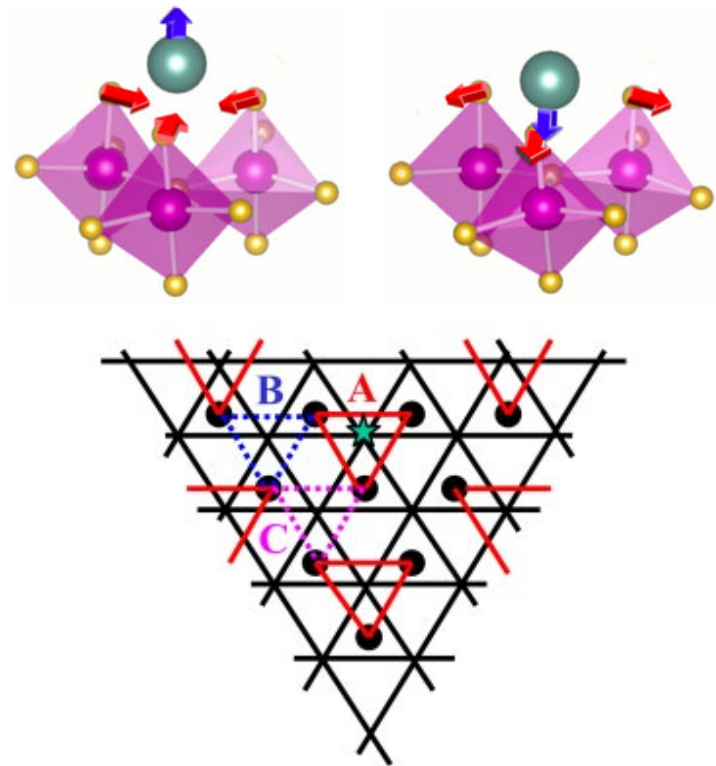
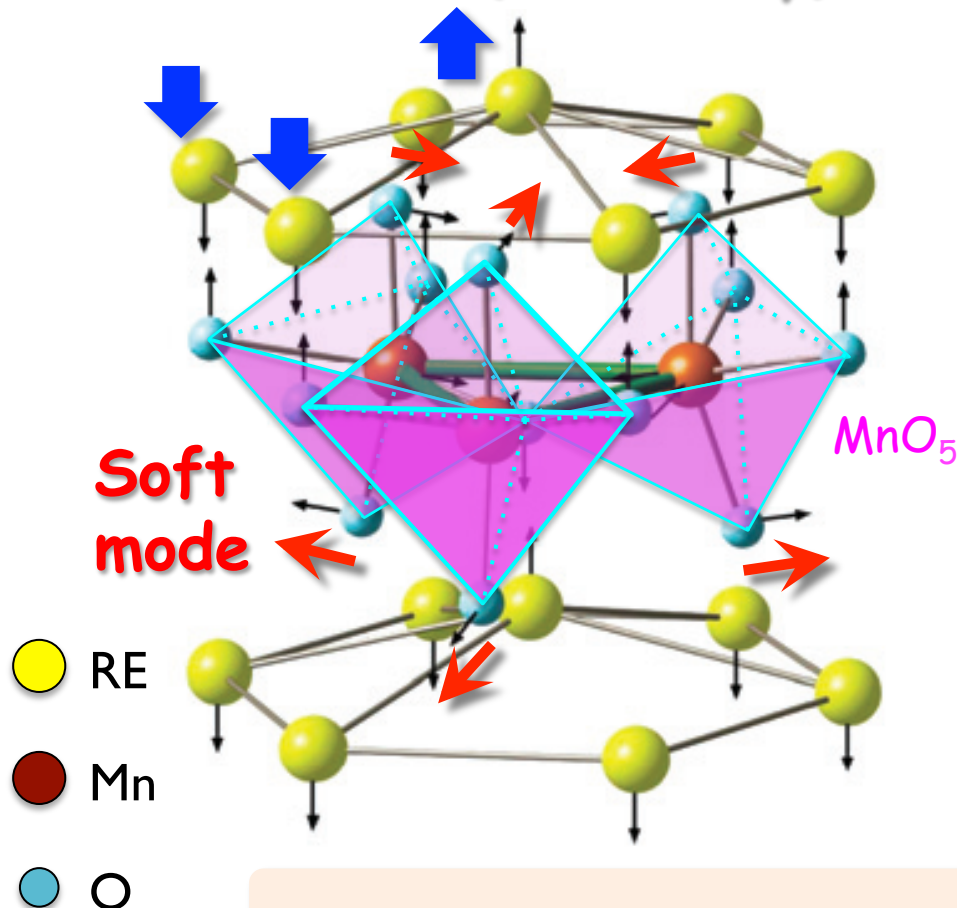
Trimerization with Z_6 symmetry breaking

Buckling of MnO_5 polyhedra accompanied by displacements of rare earth ions

→ **Ferroelectricity**

Bas B. Van Aken, et al., Nature 2004

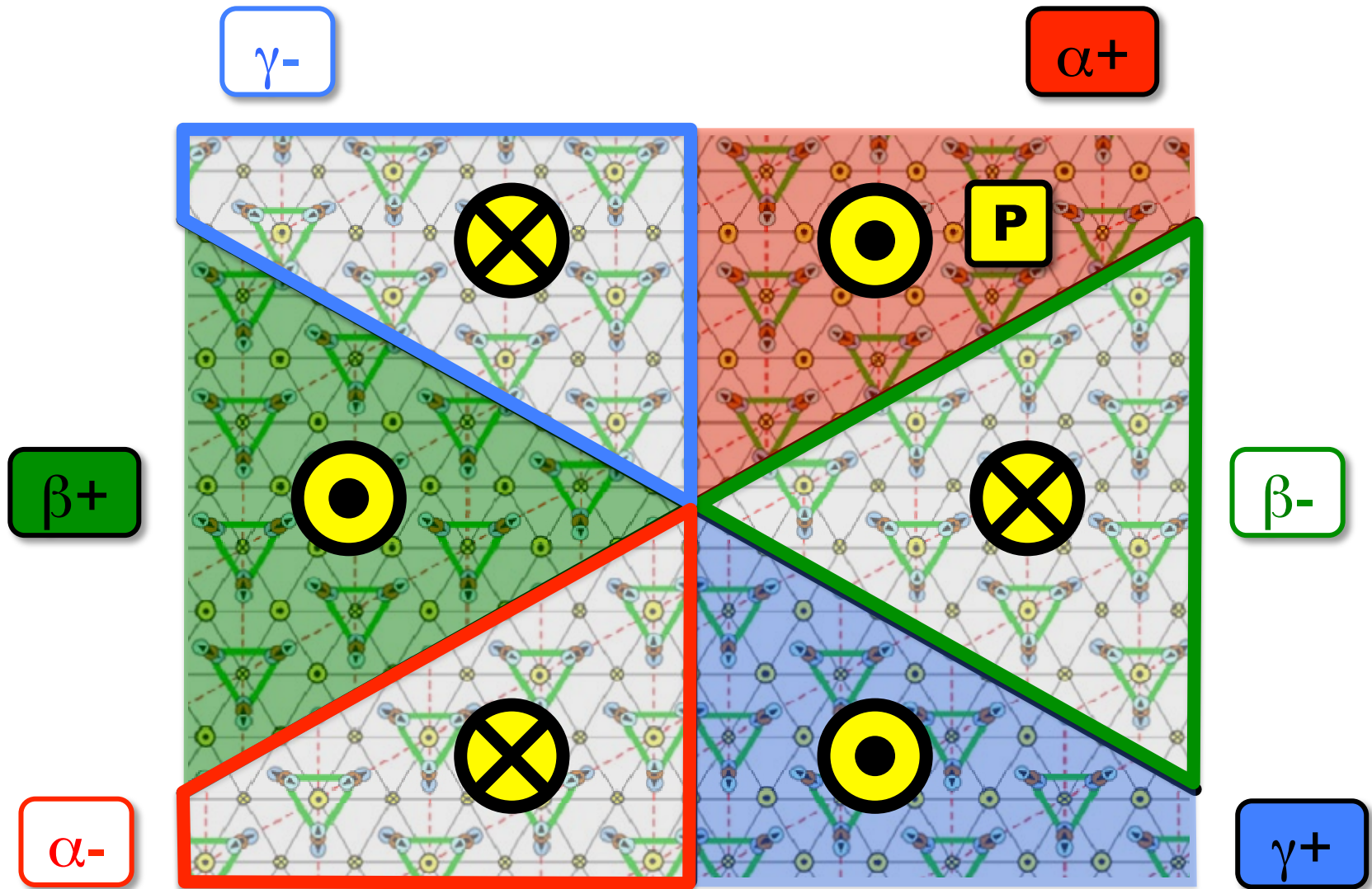
Polar mode (secondary)



6 domain types

$$Z_3 \times Z_2 = Z_6 \quad \alpha^+, \alpha^-, \beta^+, \beta^-, \gamma^+, \gamma^-$$

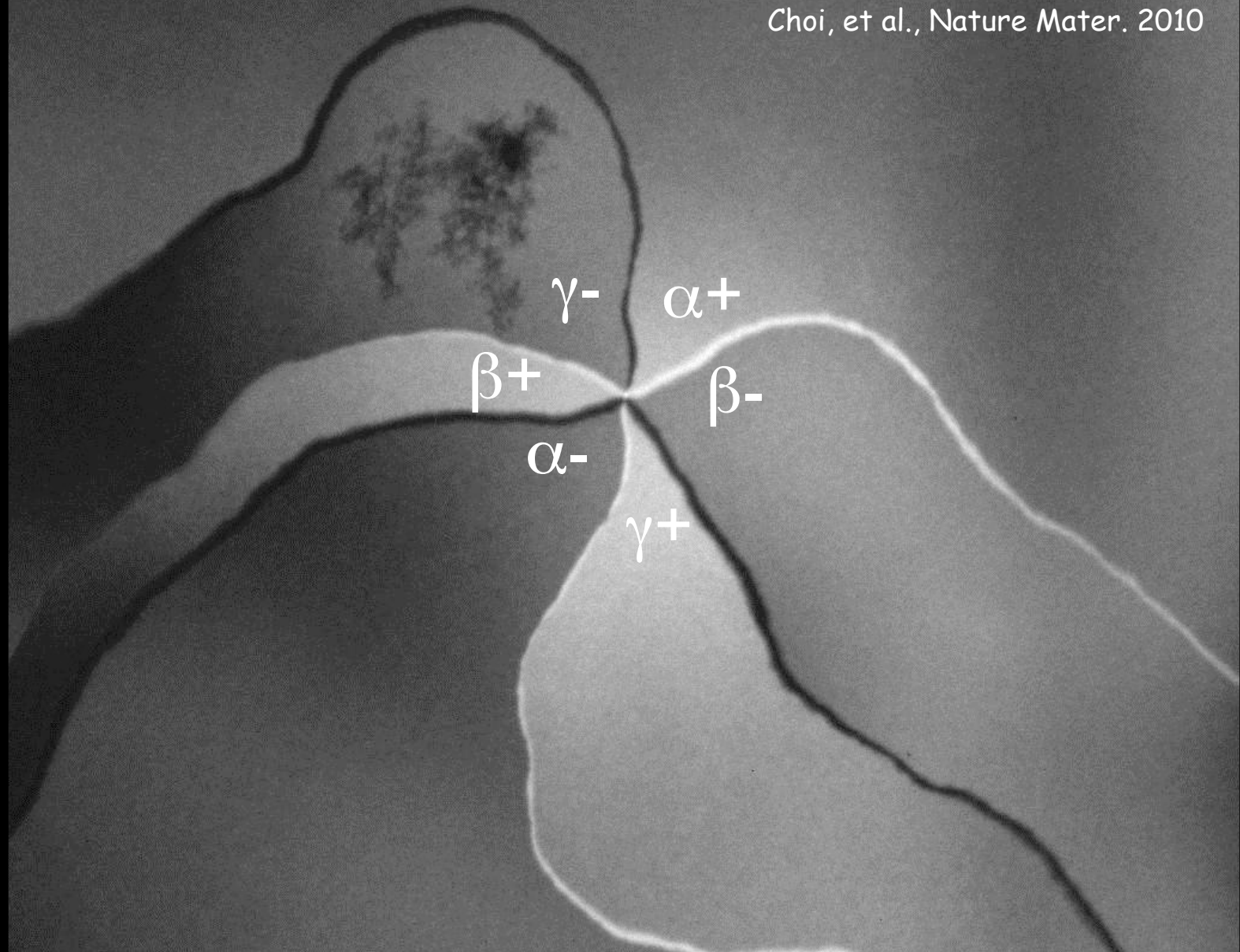
Vortex

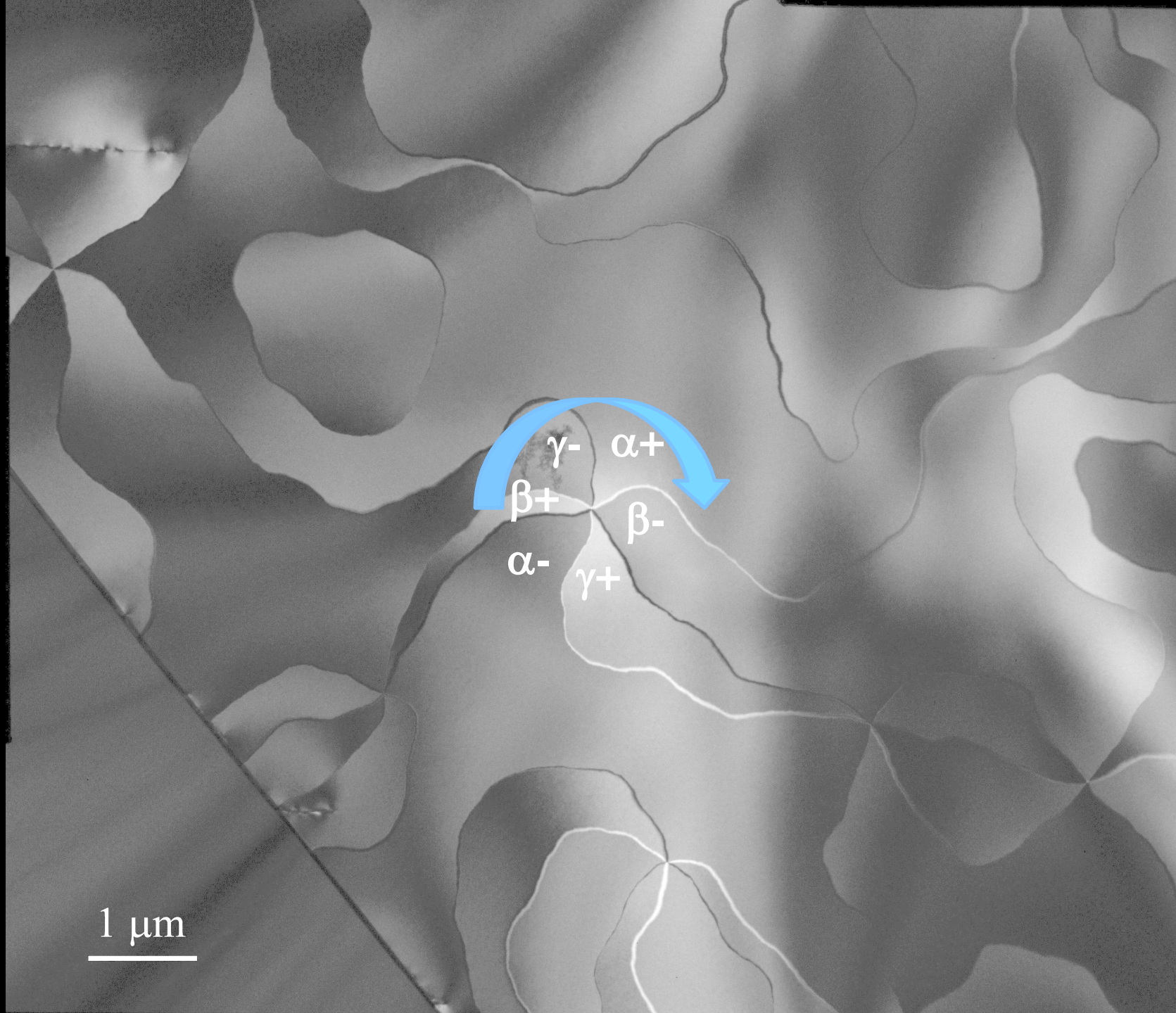


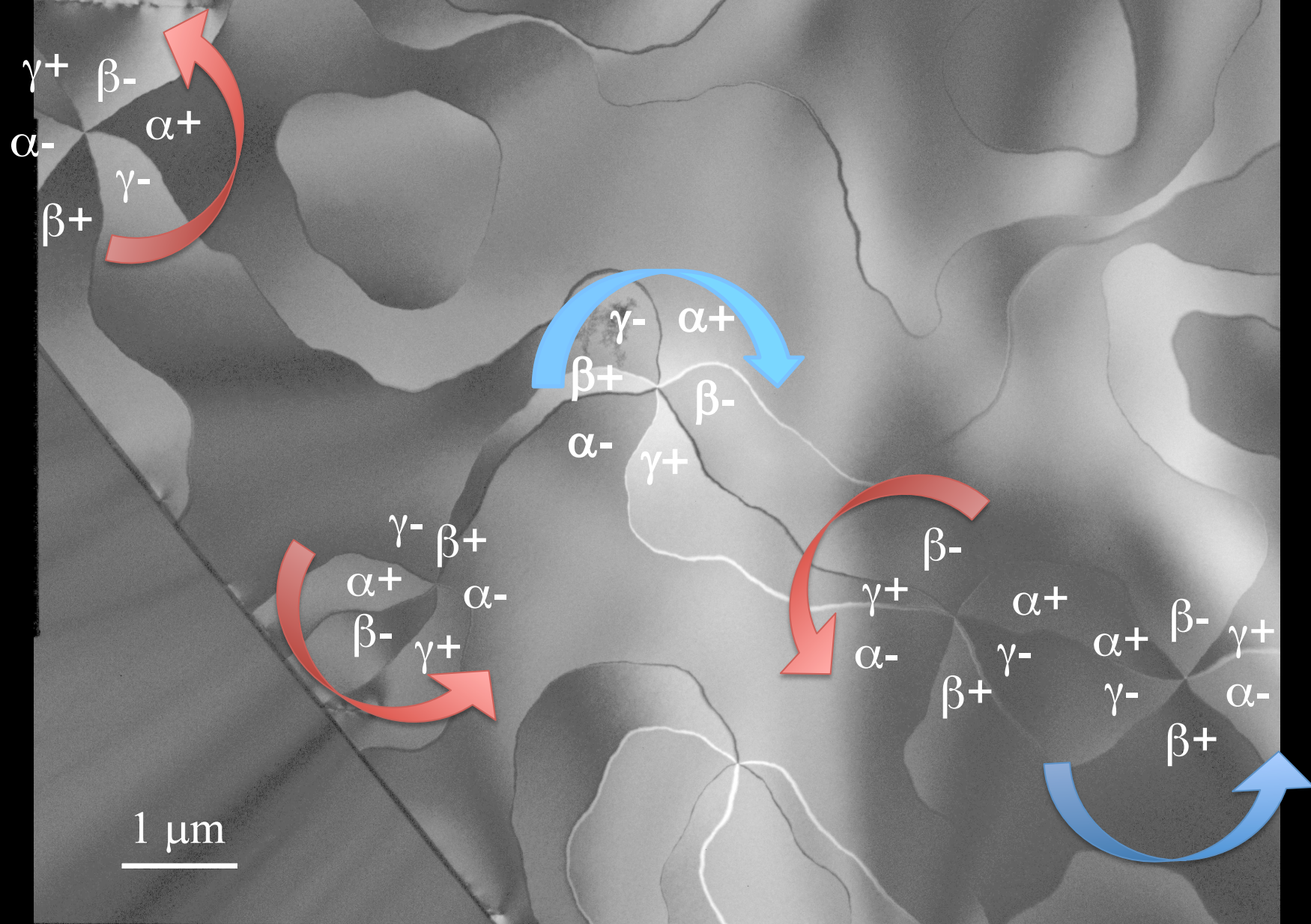
(The other types of domain walls appear to be energetically unfavorable)

TEM dark-field with (1-31) peak ($P6_3cm$)

Choi, et al., Nature Mater. 2010







Six-state "clock spin" (Z_6) model in 3D

$$\theta_i = \frac{n\pi}{3} \quad n = 0, 1, 2, 3, 4, 5$$

$$\mathcal{H} = -J \sum_{\langle ij \rangle} \cos(\theta_i - \theta_j) - J' \sum_{\langle\langle kl \rangle\rangle} \cos(\theta_k - \theta_l)$$

intra-layer **inter-layer**

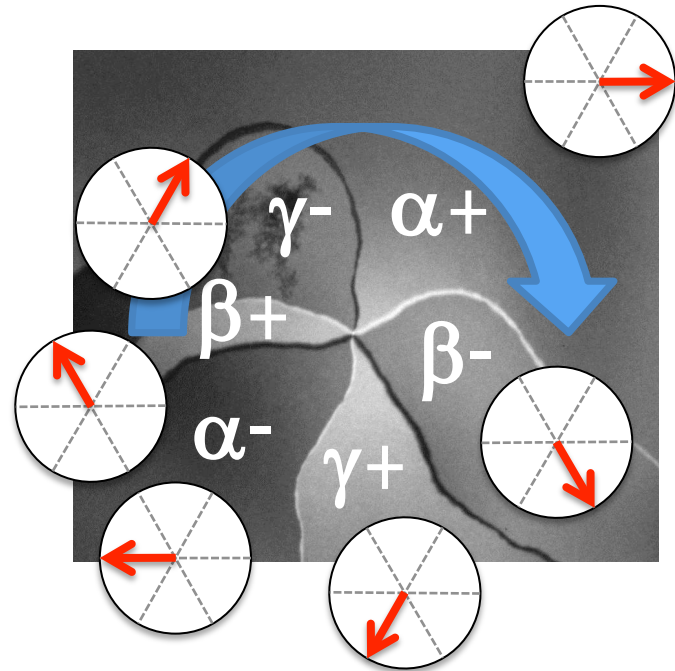
Natural model to explain the observed vortex structure

- Trimerization pattern (α, β, γ)

$$\mathbf{T}_i = (\cos 2\theta_i, \sin 2\theta_i)$$

- Electric polarization

$$\mathbf{P}_i = (\cos 3\theta_i, \sin 3\theta_i) \hat{z}$$



$$Z_6 \rightarrow U(1)$$

The Z_6 anisotropy is “dangerously irrelevant” in 3D

Blankshtein et al., PRB 1984

Oshikawa, PRB 2000

Anisotropy

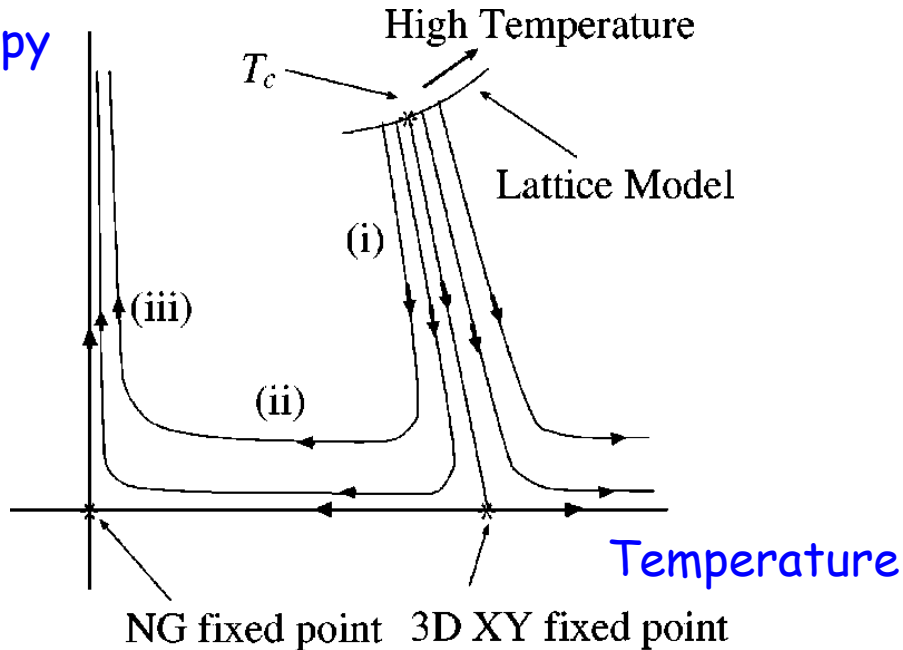
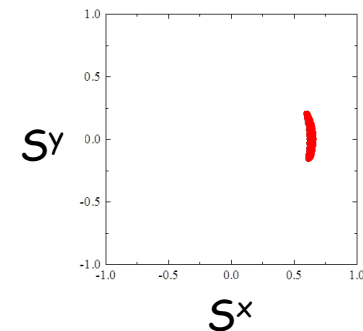
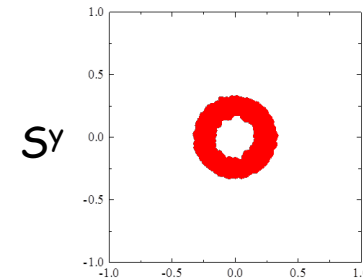
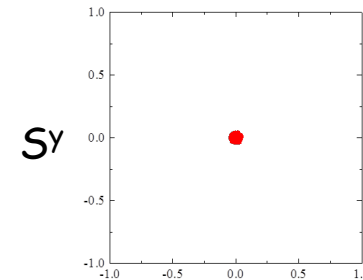
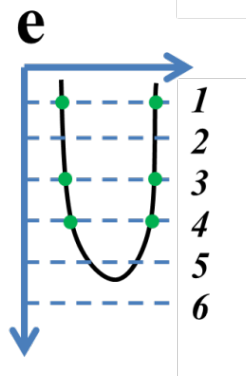
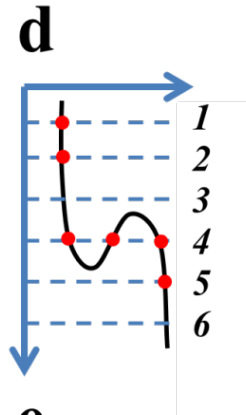
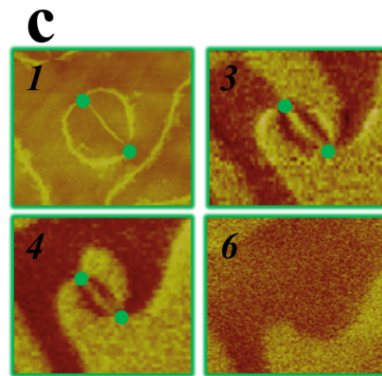
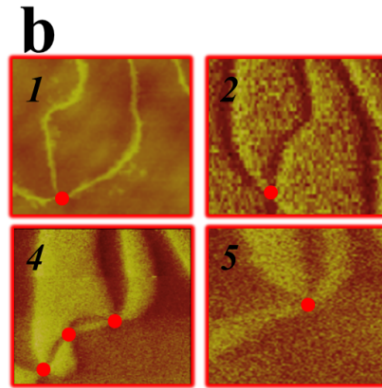
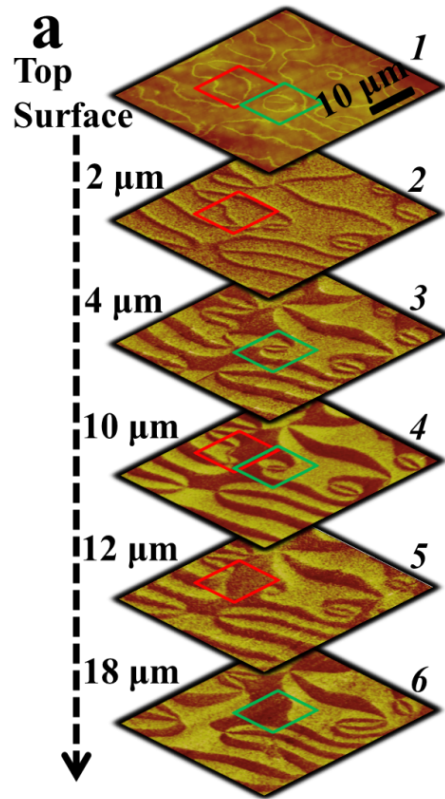


FIG. 1. The RG flow diagram of the Z_n models, projected onto the two-dimensional parameter space spanned by u and λ_n . The Z_n perturbation λ_n is irrelevant at the 3D XY fixed point, but is relevant at the NG fixed point. For T slightly less than T_c , the RG flow is divided into the three stages (i), (ii), and (iii).



Vortex loops in RMnO_3



LuMnO_3

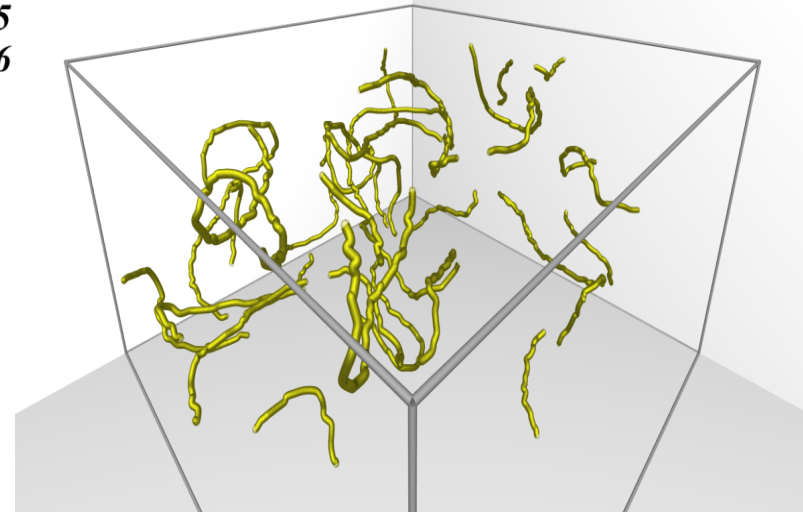


L. Onsager



R. P. Feynman

Similar idea for the superfluid transition in ^4He
[U(1) symmetry breaking]



Monte Carlo simulation 

Theory for vortices

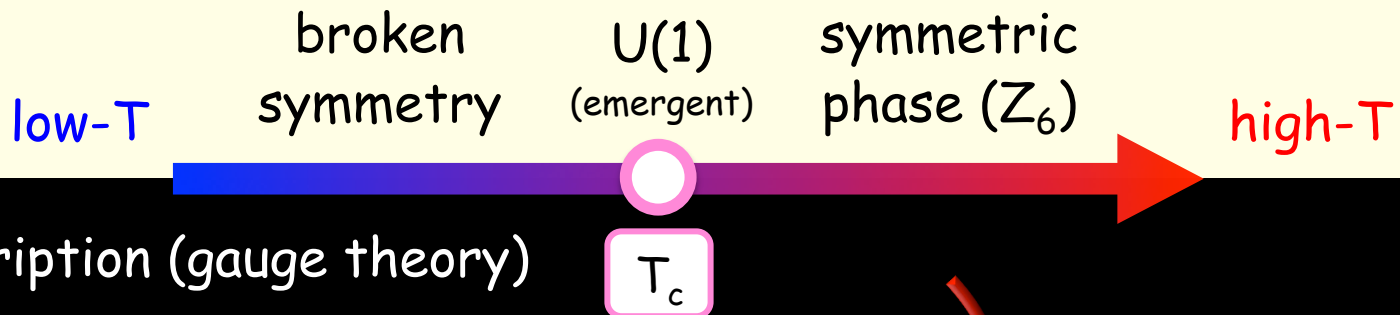
Direct description

$$\mathcal{H}_\phi = m_\phi^2 \phi^2 + u_\phi \phi^4 + \frac{1}{2} (\nabla \phi)^2$$



Kleinert, "Gauge Fields in Condensed Matter"
(World Scientific)

This may be analyzed, e.g., by the ε -expansion
cf. Wilson-Fisher fixed point

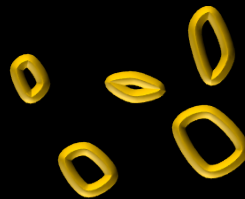


Dual description (gauge theory)

Coulomb phase

Biot-Savart coupling between
vortex-line segments

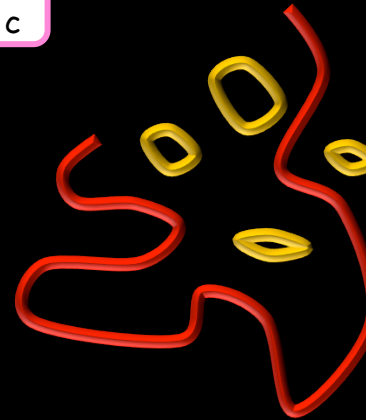
photon
(= Goldstone mode of ϕ)



Higgs phase

supercurrent of ψ
(= global vortex line of ϕ)

screening



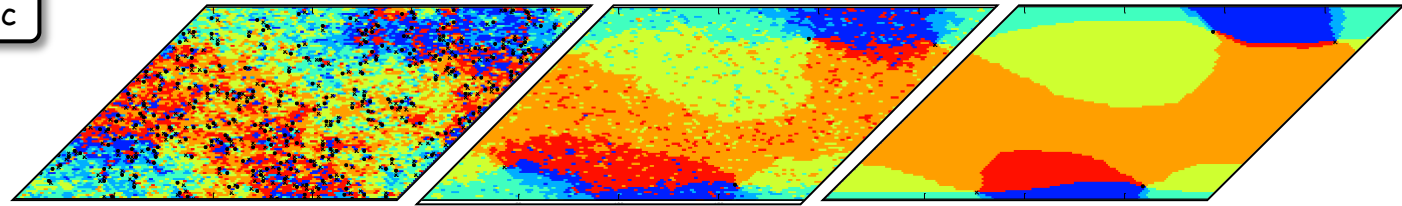
Disorder Field
Theory

$$\mathcal{H}_\psi = m_\psi^2 \psi^2 + u_\psi \psi^4 + \frac{1}{2t} \left| (\nabla - iq_{\text{eff}} \mathbf{A}) \psi \right|^2 + \frac{1}{2} (\nabla \times \mathbf{A})^2$$

Initial condition of cooling : $T_{\text{init}} > T_c$ or $T_{\text{init}} < T_c$

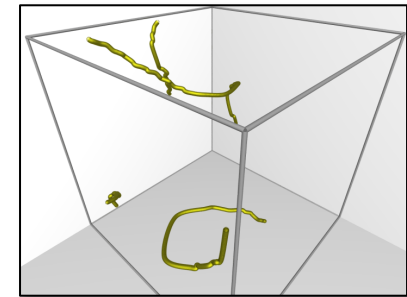
—simulation—

Cooling from $T > T_c$

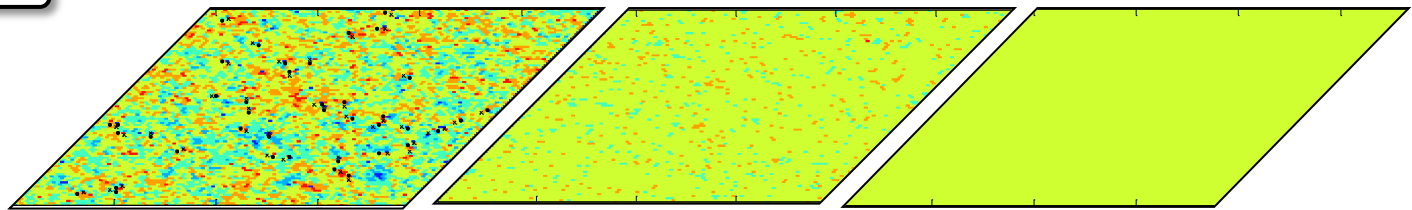
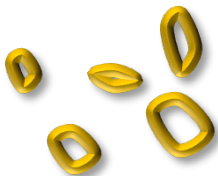


annealing

If cooled down from $T > T_c$,
percolating vortex lines remain
in the final state.



Cooling from $T < T_c$

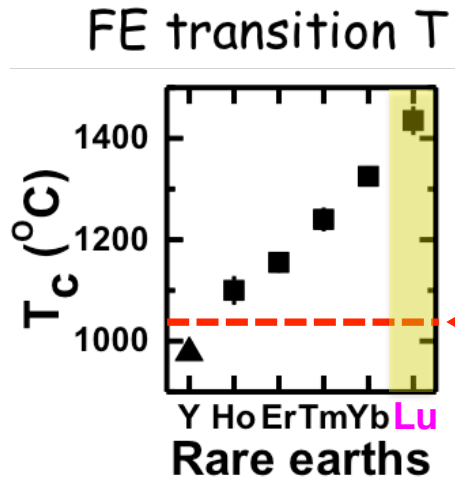


annealing

No vortex line left in the final state

Initial condition of cooling : $T_{\text{init}} > T_c$ or $T_{\text{init}} < T_c$

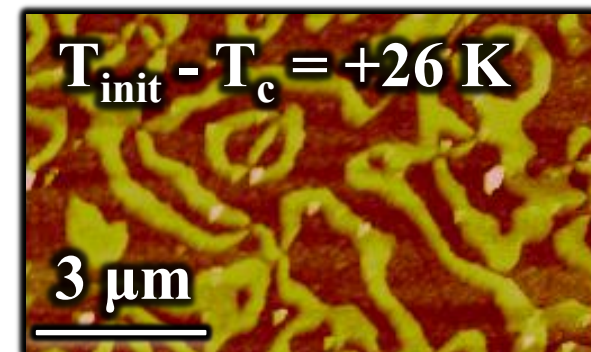
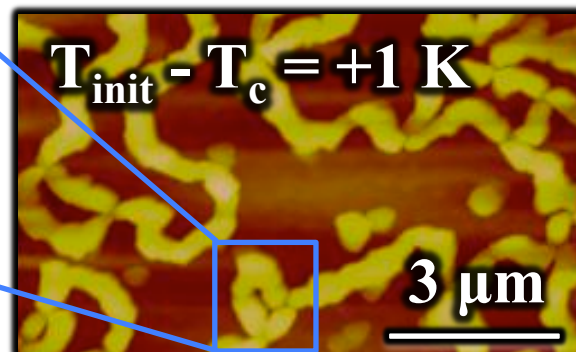
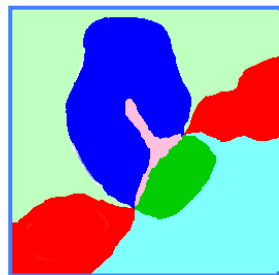
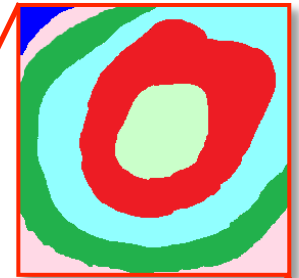
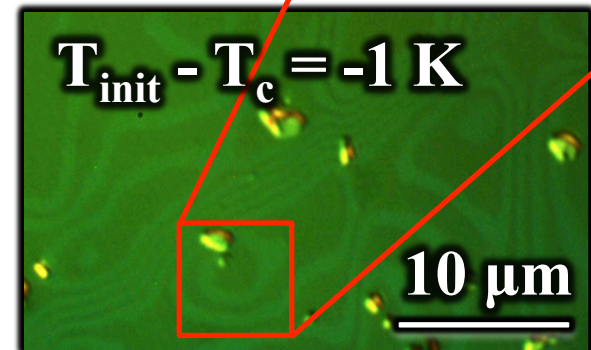
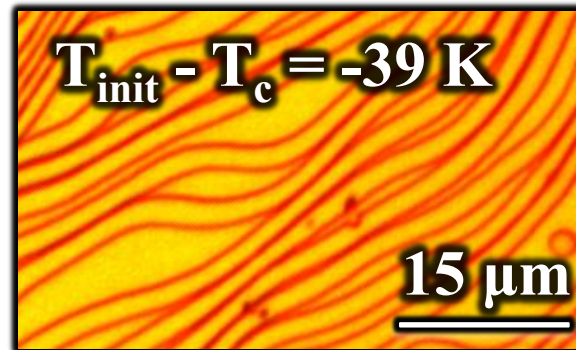
—experiments—



LuMnO_3 ($T_c = 1672$ K)

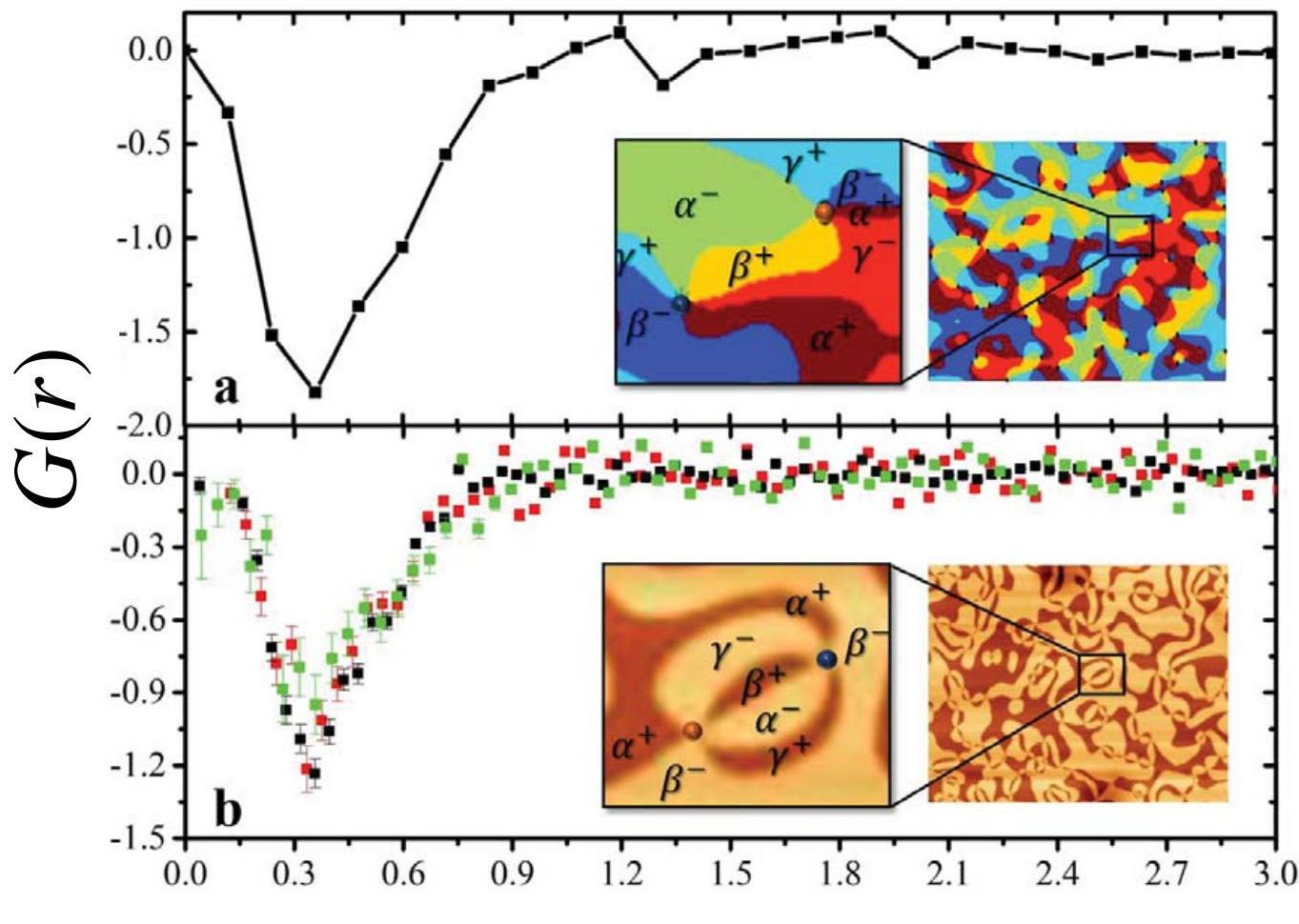
Crystal growth @ $T < T_c$

← Crystal growth temperature



Frozen vortex-antivortex pairs

$$G(r) = \langle \rho(0) \rho(r) \rangle, \quad \rho(r) = \sum_{\alpha: \text{vortex index}} q_{\alpha} \delta(r - r_{\alpha}) \quad q = +1 \text{ } (-1) \text{ for a (anti-)vortex}$$



simulation

$$T_{\text{init}} \sim 2T_c$$

$$\Delta T \sim 0.167\% \text{ of } T_c / \text{MCS}$$

$$T_{\text{fin}} = 0$$

experiments

■ ErMnO_3

■ YMnO_3

■ YbMnO_3

r/r_{avg}

Kibble-Zurek mechanism

http://en.wikipedia.org/wiki/Kibble-Zurek_mechanism

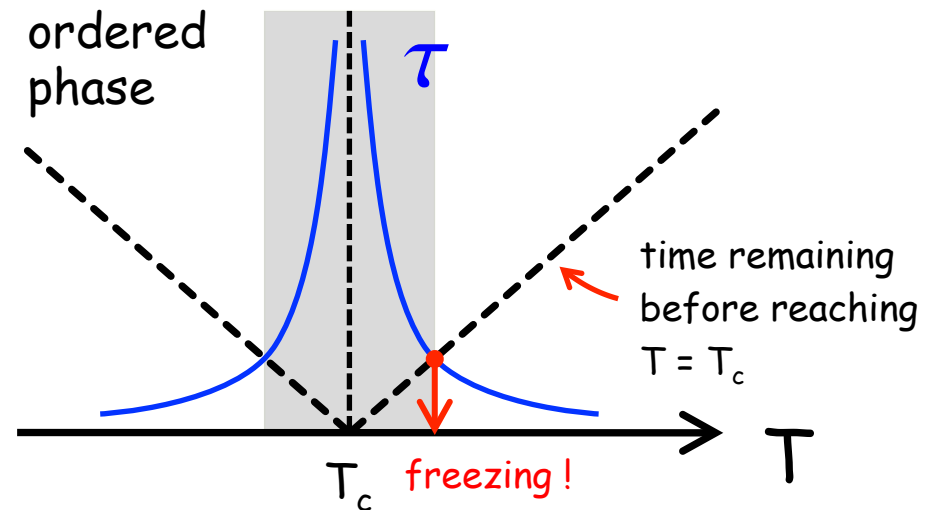
(and ref's therein)

Suppose T is lowered linearly with time (starting from $t < 0$) :

$$\varepsilon \equiv (T - T_c) / T_c = -\frac{t}{t_Q}$$

At 2nd order transitions, "critical slowing down" occurs with an exponent $z \times \nu$:

$$\tau \sim \xi^z \sim \varepsilon^{-z\nu}$$



When the relaxation time exceeds the time left to reach T_c , the dynamics becomes non-adiabatic.

Freezing condition

$$\tau = \frac{-\varepsilon}{\partial \varepsilon / \partial t} (= t_Q \varepsilon)$$

Size of frozen structures

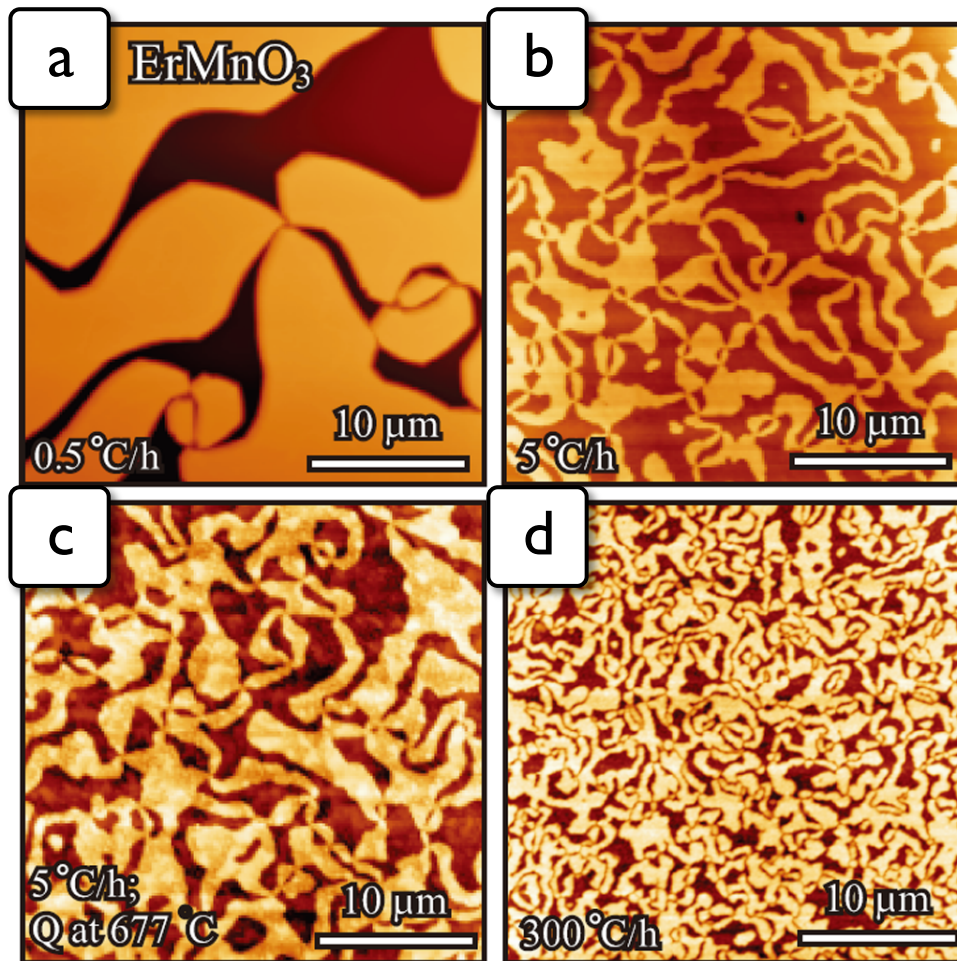
$$\xi_f \sim t_Q^{\nu/(1+z\nu)}$$

$$\varepsilon_f \sim t_Q^{-1/(1+z\nu)}$$

Cross-section density of frozen vortices

$$n_v^{\text{KZM}} \sim \frac{1}{\xi_f^2} \sim t_Q^{-\frac{2\nu}{1+z\nu}} \quad z \sim 2, \nu \sim 0.67155(27) \quad \Rightarrow \quad \frac{2\nu}{1+z\nu} \approx 0.57$$

Campostrini et al.,
PRB 2001



ErMnO_3 ($T_c = 1403$ K)

Fig	initial T	cooling rate
(a)	1493 K (+90 K)	0.5 K / h
(b)	1473 K (+70 K)	5 K / h
(c)	1473 K (+70 K)	5 K / h quench to RT @ 950 K
(d)	1473 K (+70 K)	300 K / h

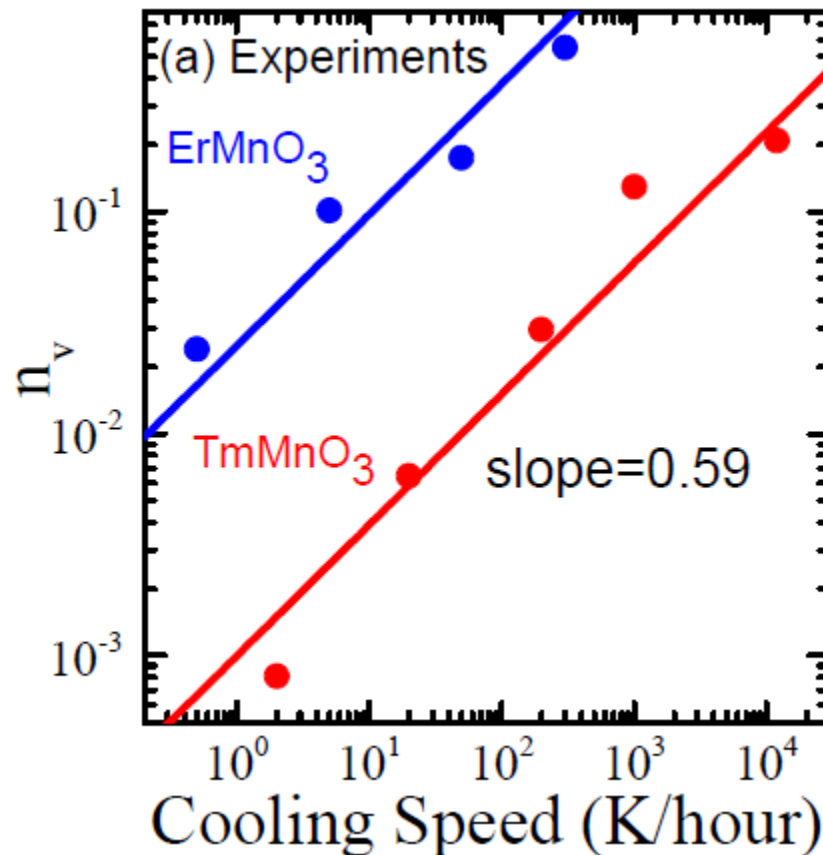
Chae et al., PRL 2012

Cross-section density of frozen vortices

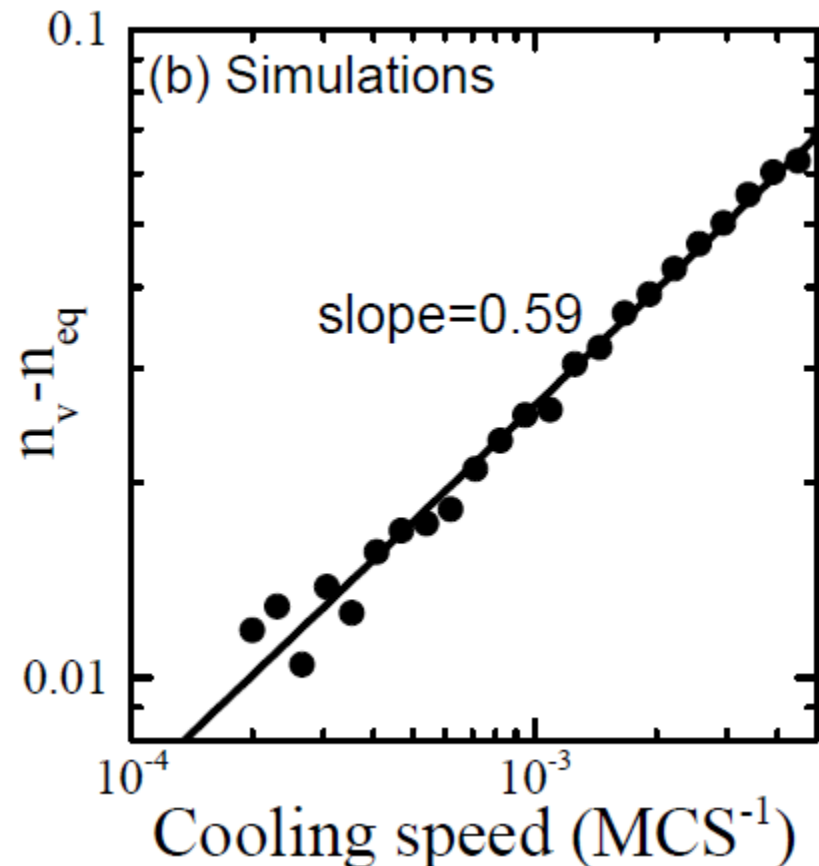
$$n_v^{\text{KZM}} \sim \frac{1}{\xi_f^2} \sim t_Q^{-\frac{2\nu}{1+z\nu}} \quad z \sim 2, \nu \sim 0.67155(27) \quad \Rightarrow \quad \frac{2\nu}{1+z\nu} \approx 0.57$$

Campostrini et al.,
PRB 2001

experiments



simulation



Summary

- Direct observation of the 3D XY transition driven by **proliferation of vortex loops** in hexagonal $RMnO_3$
- The **6-state clock model** serves as a good effective model
- The **sharp asymmetry between cooling from $T > T_c$ or $T < T_c$** is a consequence of the Higgs condensation of vortex lines
- The **Kibble-Zurek mechanism** to explain the frozen vortex density after a rapid cooling is **confirmed both in experiments and numerical simulations**